

Study on deformation behavior and strain homogeneity during cyclic extrusion and compression

Jinbao Lin · Qudong Wang · Liming Peng ·
Hans J. Roven

Received: 2 July 2008 / Accepted: 4 September 2008 / Published online: 27 September 2008
© Springer Science+Business Media, LLC 2008

Abstract In this paper, the plastic deformation behavior and strain homogeneity of the ZK60 Mg alloy during the multi-pass cyclic extrusion and compression (CEC) was simulated using the finite-element method (FEM) with a view to provide an insight into the mechanics of the process. Physical modeling (PM) experiment with same alloy was carried out to verify the results of the numerical simulations. The results show that two vortex flow regions with opposite flow direction are formed inside the cylindrical workpiece during CEC deformation. Although the deformation is inhomogeneous in both end regions of workpiece, a uniform region of equivalent strain exists, and the extent of uniform deformation increased with the increase in workpiece length.

Introduction

In the last decades, there have been considerable interests in developing severe plastic deformation (SPD) processing to fabricate bulk nanostructured metals and alloys with

unique properties [1–3]. The SPD processing is defined as a metal forming method in which extensive hydrostatic pressure is used to impose a very high strain on a bulk solid without the introduction of any significant change in the overall dimensions of the sample and having the ability to produce exceptional grain refinement [3, 4].

As a kind of continuous SPD processing, cyclic extrusion and compression (CEC) seems to be better suited for industrial applications. Moreover, it is very suitable for refining grains of hard-to-deform materials, such as Mg alloy, due to the three-dimensional compression stress imposed to the materials during the CEC processing [5]. The CEC processing was proposed by Richert and Richert [6], and it has been successfully used to produce a variety of metallic materials with ultra-fine grain structures [5–9].

The finite-element method (FEM) has been widely used to study SPD processing in order to analyze the global and local deformation responses of the workpiece with non-linear conditions of boundary, loading, and material properties [10–14]. In order to understand the refining mechanism and microstructure evolution during CEC processing, knowledge regarding the deformation behavior is essential. However, there are no reports on the plastic deformation behavior and strain distribution during CEC up to now. Hence, the aim of the present study is to investigate the deformation behavior and strain homogeneity in the multi-pass CEC using FEM and physical modeling (PM) experiments.

FEM simulation

Figure 1 shows the CEC die used in this investigation and its operation procedure. CEC was carried out by pushing a workpiece from one cylindrical chamber with a diameter D

J. B. Lin (✉) · Q. D. Wang · L. M. Peng
National Engineering Research Center for Light Alloy Net
Forming, Shanghai Jiao Tong University, Shanghai 200240,
China
e-mail: linjinbao@sohu.com

J. B. Lin
School of Applied Science, Taiyuan University of Science
and Technology, Taiyuan 030024, China

H. J. Roven
Department of Materials Science and Engineering,
The Norwegian University of Science and Technology,
7491 Trondheim, Norway

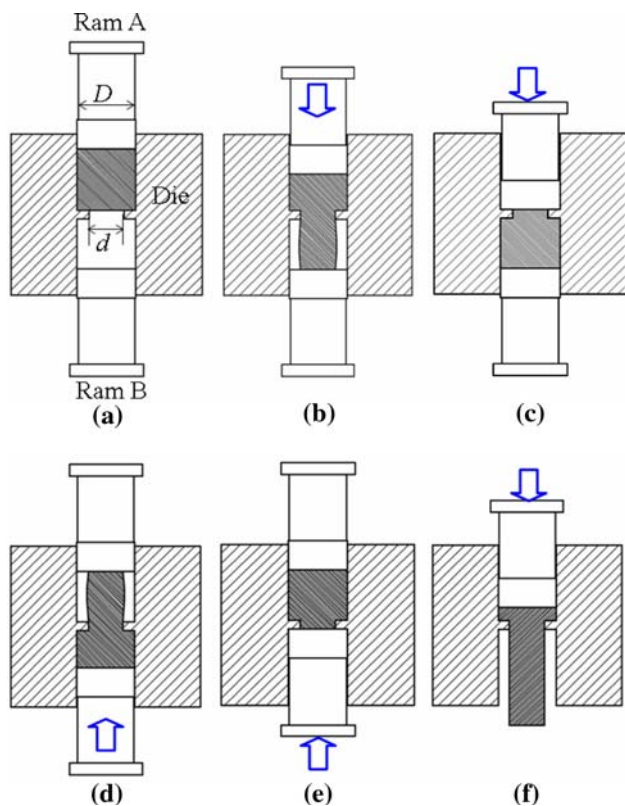


Fig. 1 Schematic diagram of the CEC facility and procedure ($D = 30$ mm, $d = 20$ mm): **a** initial state, **b** extruding with a pushing pressure on the Ram A, **c** end of Ram A, **d** reverse extruding, **e** end of Ram B, **f** final extruding to obtain a rod

into a second chamber one with equal dimensions, through a die with smaller diameter d . For the final extrusion the opposite ram is removed. In the present study, D and d are 30 and 20 mm, respectively. The as-extruded ZK60 (Mg–5.5 wt.%Zn–0.5 wt.%Zr) Mg alloy workpiece has the geometry of 29.5 mm (diameter) \times 42 mm (length).

The cylindrical die and workpiece can be simplified to an axisymmetric case, and just one-half of the longitudinal section needs to be analyzed. Figure 2 shows the axisymmetric FEM model for the simulation of the CEC process. Isothermal, two-dimensional, axisymmetric plane-strain FEM simulations of the CEC process have been carried out using the commercial finite-element software, MSC.SuperForm. In the simulations, the die and the ram can be approximately considered as rigid bodies since their strength is much higher than the workpiece's. The workpiece was modeled with 1,680 four-node isoparametric elements. Automatic remeshing was used to accommodate large deformation during the simulations. A self-adaptive step length was used as the time step of the calculation.

The most important data used in FEM simulation are the material rheology [10]. A slight modification of the material parameters has a great influence on the numerical

Fig. 2 The axisymmetric FEM model for the CEC

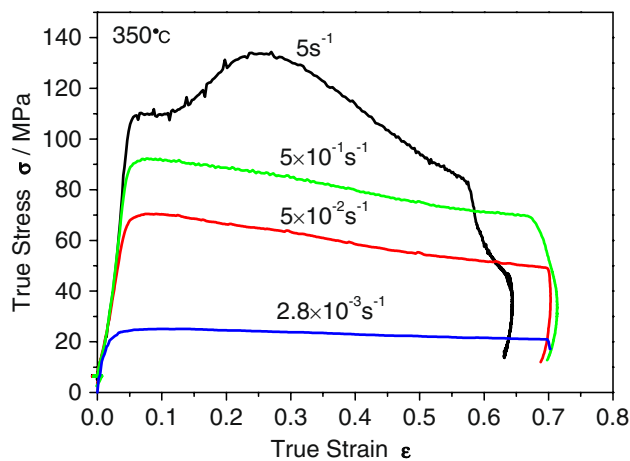
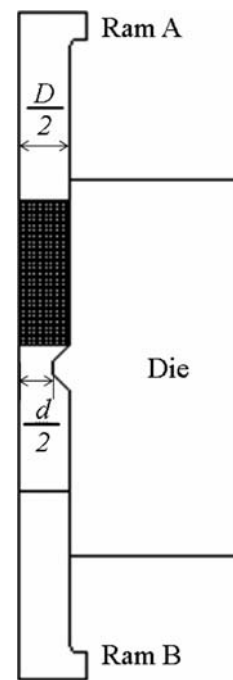


Fig. 3 The true stress–strain curves of as-extruded ZK60 alloy at 350 °C

predictions [15]. In order to obtain results with a high degree of confidence, the material rheology for the studied alloy was defined by compression stress–strain curves, which were measured by a Gleeble 3500 machine using 10 mm (diameter) \times 15 mm (length) samples at 350 °C, as shown in Fig. 3. In the simulation, a constant ram speed of 8 mm/s was imposed. The friction between the workpiece and the CEC die was assumed to obey Coulomb's law and a friction coefficient of 0.2. During the experiments, the temperature varies between 340 and 360 °C, but for simplicity, the self-heating of the workpiece was not considered here. At the same time, isothermal conditions were assumed and the temperature was set to 350 °C. The database of former pass simulation was loaded into the

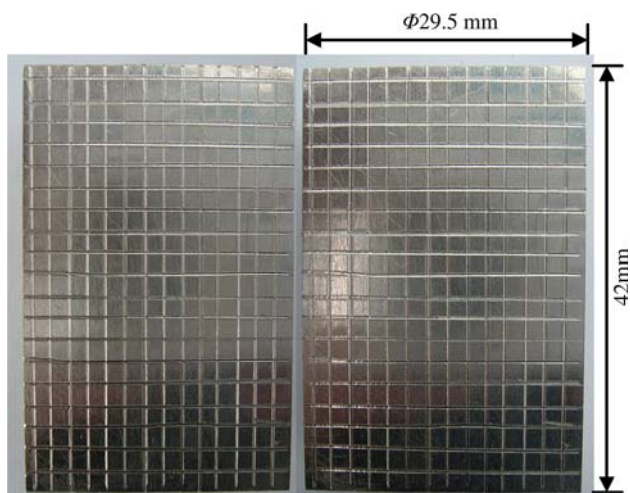


Fig. 4 The semi-cylindrical ZK60 alloy workpiece for PM experiment, the longitudinal sections are scribed with perpendicular lines

pre-processor for the next pass simulation. CEC processing simulation was carried out up to 12 passes.

PM experiment

PM is a technique used to simulate plastic flow of metal in real metal forming operations [16]. For the sake of validation of the results of the FEM simulations, PM experiment was carried out using an extruded ZK60 alloy workpiece [3], with the same shape as in the FEM simulation. The CEC facility and deformation procedure is also similar to the FEM simulation. In order to study the plastic flow of the ZK60 alloy during the process, the cylindrical workpiece was cut into two semi-cylindrical workpieces along the cylinder axis using electric spark machining, and then the longitudinal sections were scribed with perpendicular grid lines, as shown in Fig. 4. The CEC process was carried out by pushing the two semi-cylindrical pieces together in the cylindrical chamber of the CEC die at 350 °C. Graphite was used as lubricant.

Results and discussion

Plastic deformation behavior

In order to better visualize the metal flow in the workpiece during the forming process, it is useful to examine lines that can be considered to be scribed onto the material [17], as shown in Fig. 5. In this work, the plastic deformation behavior during CEC was explained by using the flow lines. Before CEC processing (Fig. 5, 0 P), the lines are perpendicular in both simulation and experiment. After two

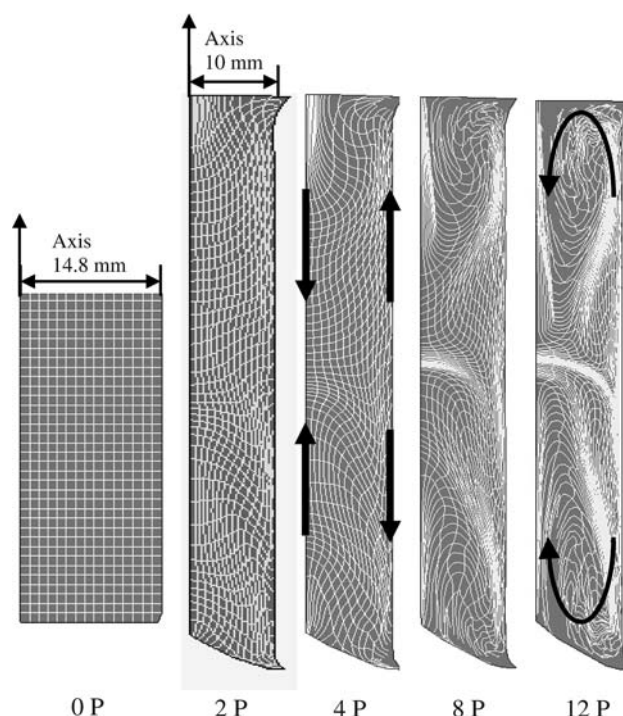


Fig. 5 Flow lines in the workpiece before CEC (0 P) and after CEC processing (2, 4, 8, and 12 passes) of the FEM simulation, black arrows represent the metal flow direction

and four passes of CEC, it can be seen that the metal flow direction is opposite in the center and the surface of the workpiece, as shown in the Fig. 5, 4 P. The black arrows represent the metal flow direction. After larger deformation, such as 8 and 12 passes, two vortex flow regions with opposite flow directions are formed inside the workpiece.

Figure 6 shows the comparison of the flow lines in the workpiece between PM experiment and FEM simulation after 12-pass CEC processing at 350 °C. As shown in Fig. 6a, after CEC processing, the lines scribed on the longitudinal sections of the workpiece were severely distorted. It implies that the workpiece suffered SPD during CEC processing. Similar to FEM results (Fig. 6b), two vortex flow regions are formed inside the PM workpiece during CEC processing. Moreover, the FEM simulation results are validated by the PM experiment.

Equivalent plastic strain/effective strains

The grain refinement during CEC processing is dependent on the accumulated strain in the workpiece after the final pass. Moreover, to a certain extent, the homogeneity of the microstructure relies on the distribution of strains. Figure 7 shows the total equivalent plastic strain (TEPS) distribution in the workpiece after CEC processing. It shows that the TEPS distribution is inhomogeneous in the two end regions of the 2-pass workpiece. The strains of both end regions are

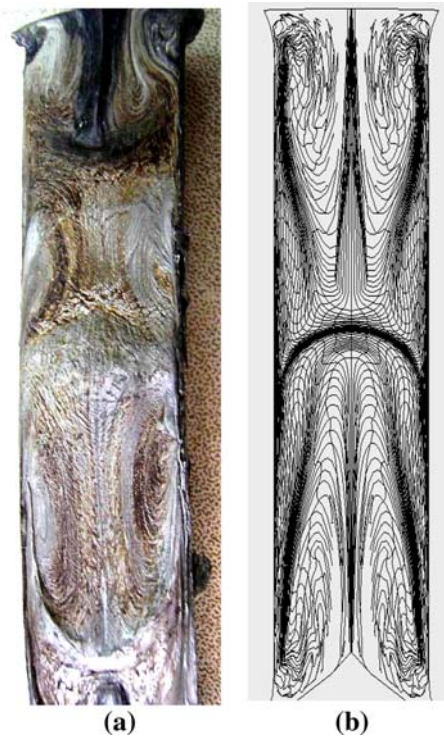


Fig. 6 Comparison of flow lines result of **a** PM and **b** FEM result after 12-pass CEC processing at 350 °C

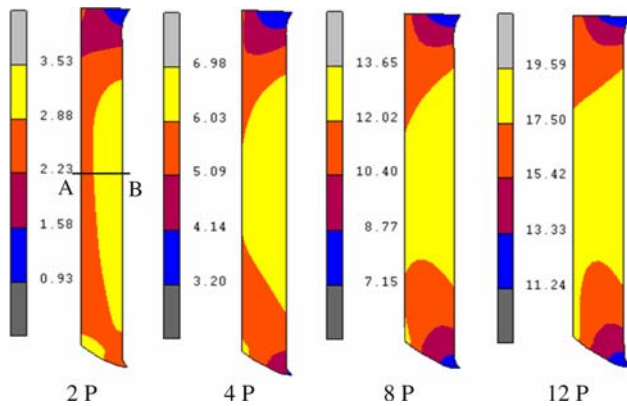


Fig. 7 Distribution of the total equivalent strain during the CEC processing after 2, 4, 8, and 12 passes

lower than that of the center region. Moreover, the distribution does not vary with the increase in CEC pass number. A general expression for the equivalent strain ϵ generated in the workpiece after n -pass CEC processing which was obtained by Richert et al. [6, 8, 18] is given by the following equation:

$$\epsilon = 2(2n - 1) \ln \frac{D}{d} \tag{1}$$

According to Eq. 1, the equivalent strains are 2.43, 5.67, 12.15, 18.63 for 2, 4, 8, 12 passes of CEC processing in this work ($D = 30$ mm, $d = 20$ mm). To obtain quantitative

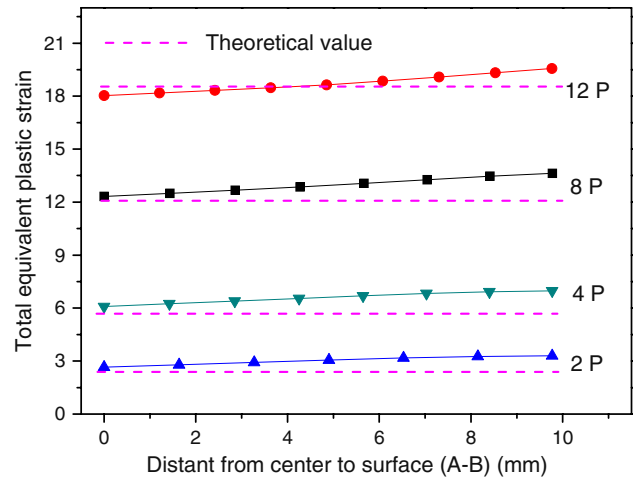


Fig. 8 Variation curves of TEPS from center to surface (cross the width $A-B$)

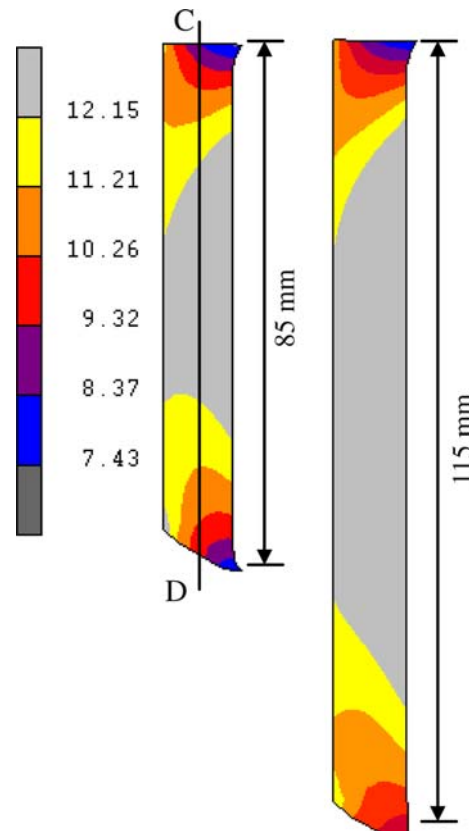


Fig. 9 Distribution of the TEPS of two workpieces with different lengths after 8-pass CEC

information regarding the strain homogeneity, the TEPS is plotted across the width ‘ $A-B$ ’ at the center of the workpiece in Fig. 8. The location of ‘ $A-B$ ’ is shown in Fig. 7. The TEPS value of ‘ $A-B$ ’ obtained in the simulation is somewhat higher than the theoretical value obtained by

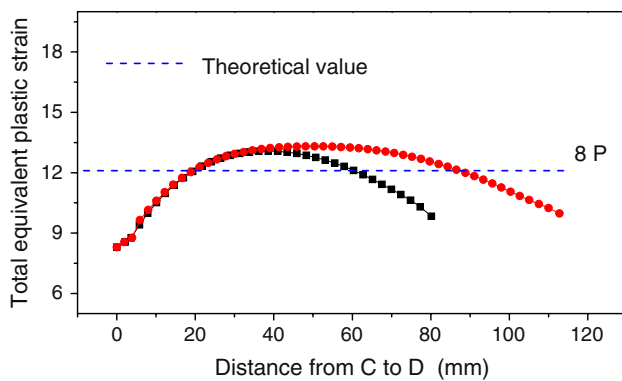


Fig. 10 Variation curves of TEPS from one end to another (*C–D*) of two workpiece

Eq. 1. From center to surface (*A–B*), the value of TEPS increased about 1.0 for all passes.

The inhomogeneous distribution of TEPS in both end regions of the workpiece after CEC processing is similar to the Saint-Venant end effects [19]. Therefore, to obtain more material with uniform strain after CEC processing, it is useful to lengthen the workpiece. Figure 9 shows the TEPS distribution in a simulation of two workpieces with different lengths after the 8-pass CEC processing at 350 °C. Figure 10 shows the TEPS value of two workpiece along '*C–D*,' its location is shown in Fig. 9. It clearly shows that the uniform strain region is extended with the increase in workpiece length.

Conclusions

The plastic deformation behavior and strain homogeneity of ZK60 Mg alloy during a multi-pass CEC at 350 °C was investigated using FEM and PM experiment with a view to provide an insight into the mechanics of the process. The main conclusions are as follows:

- (1) The FEM results were verified by PM experiment. Results show that two vortex flow regions with opposite flow direction are formed inside the ZK60 alloy workpiece after CEC processing.
- (2) The TEPS distribution is inhomogeneous in the two end regions of the workpiece. The strains of both end regions are lower than that of the center region.

Moreover, the strain distribution is invariable to the increase of CEC pass numbers, which is similar to the Saint-Venant end effects.

- (3) Longer ingots should be used to get more materials with uniform strain during the CEC process.

Acknowledgements This work was supported by the National Natural Science Foundation of China (No. 50674067), National Basic Research Program of China (No. 2007CB613701) and Program of Shanghai Subject Chief Scientist (No. 08XD14020). Special thanks to Snorre Kjørstad Fjeldbo for useful comments on the manuscript.

References

1. Valiev RZ, Islamgaliev RK, Alexandrov IV (2000) Prog Mater Sci 45:103. doi:10.1016/S0079-6425(99)00007-9
2. Valiev RZ, Estrin Y, Horita Z, Langdon TG, Zehetbauer MJ, Zhu YT (2006) JOM 58(4):33. doi:10.1007/s11837-006-0213-7
3. Lin JB, Wang QD, Peng LM, Peng T (2008) Mater Trans 49:1021. doi:10.2320/matertrans.MC200766
4. Valiev RZ (2007) J Mater Sci 42:1483. doi:10.1007/s10853-006-1281-3
5. Wang QD, Lin JB, Peng LM, Chen YJ (2008) Acta Metall Sinica 44(1):55
6. Richert J, Richert M (1986) Aluminium 62(8):604
7. Lin JB, Wang QD, Peng LM, Roven HJ (2008) J Alloys Compd. doi:10.1016/j.jallcom.2008.09.031
8. Richert M, Liu Q, Hansen N (1999) Mater Sci Eng A 260:275. doi:10.1016/S0921-5093(98)00988-5
9. Lee SW, Yeh JW (2005) Metall Mater Trans A 36:2225. doi:10.1007/s11661-005-0341-7
10. Petrescu D, Savage SC, Hodgson PD (2002) J Mater Process Technol 125–126:361. doi:10.1016/S0924-0136(02)00301-1
11. Nagasekhar AV, Kim HS (2008) Comput Mater Sci. doi:10.1016/j.commatsci.2008.02.030
12. Zhao WJ, Ding H, Ren YP, Hao SM, Wang J, Wang JT (2005) Mater Sci Eng A 410–411:348. doi:10.1016/j.msea.2005.08.134
13. Dumoulin S, Roven HJ, Werenskiold JC, Valberg HS (2005) Mater Sci Eng A 410–411:248. doi:10.1016/j.msea.2005.08.103
14. Tham YW, Fu MW, Hng HH, Yong MS, Lim KB (2007) J Mater Process Technol 192–193:121. doi:10.1016/j.jmatprotec.2007.04.030
15. Gavrus A, Massoni E, Chenot JL (1996) J Mater Process Technol 60:447. doi:10.1016/0924-0136(96)02369-2
16. Rosochowski A, Olejnik L (2002) J Mater Process Technol 125–126:309. doi:10.1016/S0924-0136(02)00339-4
17. MSC.Superform 2005, Command reference manual
18. Richert M, Korbela A (1995) J Mater Process Technol 53:331. doi:10.1016/0924-0136(95)01990-V
19. Choi I, Horgan CO (1977) J Appl Mech 44:424